

Scattering of 10.4 MeV polarized neutrons from bismuth and lead between 2° and 65° *

A. H. Hussein,[†] J. M. Cameron, S. T. Lam, G. C. Neilson, and J. Soukup
*Nuclear Research Centre, Department of Physics,
 University of Alberta, Edmonton, Alberta, Canada*

(Received 19 July 1976)

The polarization and differential cross sections for the scattering of 10.4 MeV neutrons from lead and bismuth are measured from 1.5° to 65° . No significant differences are found between the polarizations in the scattering at small angles in contrast to the situation reported at 2.45 MeV. The data over the complete angular range are reproduced using a standard optical potential with the addition of the long-range interaction between the neutron magnetic moment and the nuclear Coulomb field.

[NUCLEAR REACTIONS Pb, Bi(n, n), $E_n = 10.4$ MeV; measured $\sigma(\theta)$ and $P(\theta)$; $\theta = 1.5^\circ - 65^\circ$; DWBA analysis.]

I. INTRODUCTION

The interaction of the magnetic moment of neutrons with the Coulomb field of a nucleus (the Mott-Schwinger interaction) has been extensively studied since its existence was first pointed out by Schwinger.¹ There is, in addition, a weaker interaction between the induced electric moment of the neutron and the electric field of the nucleus. The observation of this latter interaction has also been claimed but this is still controversial, both positive² and negative³ results being reported recently. The situation was further complicated by the publication of systematic differences in the polarization for scattering from lead and bismuth at 2.45 MeV.⁴ This difference is not expected if one uses an optical model potential together with the above long-range electromagnetic forces. It may thus indicate the existence of an additional long-range force, such as an interaction between the magnetic moment of the neutron and that of the nucleus. (Bismuth has spin $\frac{9}{2}$, while lead is a mixture of spin 0 and spin $\frac{1}{2}$ nuclei.)

The effect of the Mott-Schwinger interaction dominates the differential cross section only at angles below about 2° , whereas its effect on the polarization extends to beyond 10° . Nuclear effects usually dominate the differential cross section in the measurable range and one can look for sensitivity to differing optical potentials. A recent report⁵ on scattering of 7–14 MeV neutrons by nuclei in the range $2.5^\circ - 15^\circ$ indicates that the cross-section data can be reproduced by the local potential given by Wilmore and Hodgson⁶ and that the predictions are sensitive to different potential parameters. It is thus of interest to see if the potential which fits the small angle cross section

can also predict correctly the polarization and differential cross section over an extended angular range.

In the present work we report measurements on the scattering of polarized 10.4 MeV neutrons from bismuth and lead between 1.5° and 65° . The results are compared to calculations which include the basic Mott-Schwinger plus nuclear interaction at small angles. Predictions obtained from three commonly used optical potential sets are compared to the larger angle data.

II. EXPERIMENTAL PROCEDURE

The reaction ${}^9\text{Be}(\alpha, n){}^{12}\text{C}$ was used to produce 10.4 ± 0.25 MeV neutrons with polarization of 0.44 ± 0.03 ⁷ at the laboratory reaction angle of 30° . Pulses of 5.45 MeV α particles produced by the University of Alberta 7.5 MeV van de Graaff accelerator were used to bombard targets prepared by evaporating beryllium onto 0.038 cm thick tantalum backings. Targets used were always less than 0.8 mg/cm, i.e., less than 500 keV for an α energy of 5.45 MeV. These targets, cooled by blowing air on the backing, were able to withstand beam currents of 3 μA for several days. Under these conditions a neutron flux of about 6×10^6 neutrons/sec $\mu\text{A sr}$ was obtained. The analyzing power for the scattering of the polarized neutrons was determined by measuring the scattering cross section at a given angle for incident neutrons with spin up and spin down. A superconducting solenoid⁸ was used to rotate the neutron spin vector by 180° . The solenoid was enclosed in a liquid helium cryostat which had a room temperature air bore 3.8 cm in diameter, along the axis of the solenoid.

Combinations of source and detector shielding

were used in different configurations to allow measurements to be made over the angular range of 1.5° – 65° . The geometry used for small angle measurements is shown in Fig. 1. Good beam collimation and angular resolution were obtained by using the normal source and detector shielding together to form a long collimator. In this mode the scatterer was 3.0 m away from the source, and consequently the incident neutron flux was very low. To compensate for this, three detectors were used simultaneously to detect neutrons scattered at different angles. This, together with the large scattering cross sections in the small angle region, made it possible to reduce the total data collection time to a reasonable level. In the large angle configuration, shown in Fig. 2, the scatterer was placed closer to the source and a single detector was placed inside the detector shield which could be rotated around the scatterer.

Scatterers used were solid cylinders of lead or bismuth 7.6 cm high and 2.5 cm in diameter. All the neutron detectors were NE213 liquid scintillators. In the small angle measurements the detectors were cylinders each 7.6 cm high and 5.08 cm in diameter with their axes perpendicular to the reaction plane. These cylinders were coupled to RCA 8575 photomultipliers. The detector used in the large angle measurements was a cylinder, 5.08 cm long and 8.89 cm in diameter, with its axis in the reaction plane. This was coupled to an RCA 4522 photomultiplier. An identical detector, used as a monitor for all measurements, detected neutrons emitted from the source at zero degrees.

Standard time-of-flight (TOF) and neutron- γ (n - γ) discrimination techniques were used to handle detector signals. The analog outputs of two time-to-amplitude converters, one for n - γ discrimination and the other for TOF, were digitized by analog-to-digital converters and fed to a Honeywell DDP-516 computer. Digital windows were set on the "neutron peak" and the " γ peak" of the n - γ

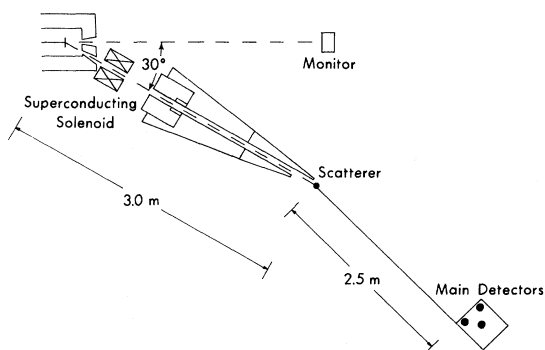


FIG. 1. Experimental setup for small angle measurements.

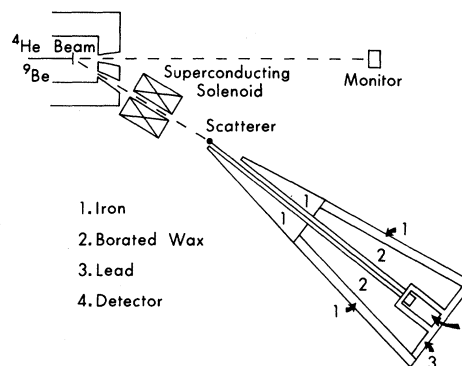


FIG. 2. Experimental setup for large angle measurements.

spectrum. An on-line computer program was used to sort the TOF spectrum accordingly.

The direction of the incident neutron beam was determined by sweeping the detector through the beam and measuring the fraction of the flux absorbed in the scatterer at different positions. The center of the absorption curve was taken as the

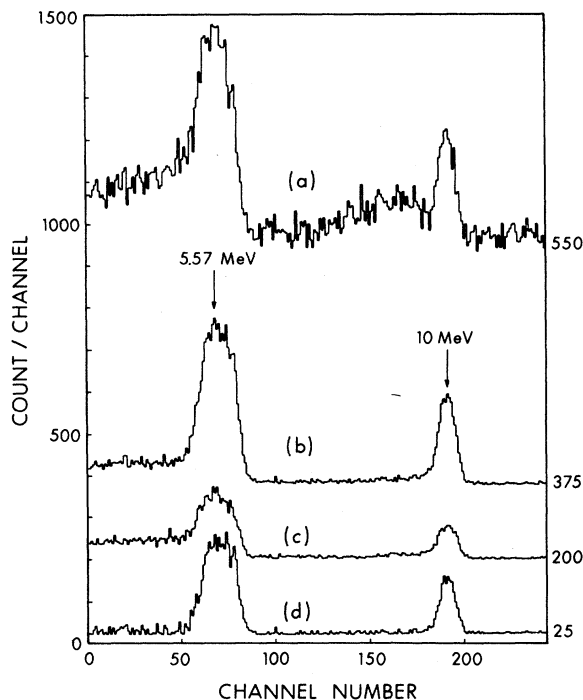


FIG. 3. Typical time-of-flight spectra for the elastic scattering of polarized neutrons from Pb at a scattering angle of 1.5° : (a) raw spectrum taken with scatterer in, (b) scatterer-in spectrum after γ separation, (c) scatterer-out spectrum after γ separation, (d) in-out spectrum. Each spectrum is offset by a certain amount, so that the number indicated at the right must be subtracted from the ordinate to obtain the correct magnitude.

direction of the incident beam from which the angular position of the detector could be measured. The uncertainty in determining this position gave rise to an uncertainty in the detector position of $\pm 0.13^\circ$. The angular resolution was $\pm 0.6^\circ$ for small angle measurements and $\pm 0.9^\circ$ for large angle measurements.

The spectra were normalized to the monitor and scatterer-out spectra were then subtracted from corresponding scatterer-in spectra. Figure 3 shows typical time-of-flight spectra for neutrons scattered from Pb at a laboratory scattering angle of 1.5° . The 5.57 MeV neutrons are from the reaction ${}^9\text{Be}(\alpha, n_1){}^{12}\text{C}^*(4.43 \text{ MeV})$.

Multiple scattering and finite geometry corrections were determined using a modified version of the Monte-Carlo code PMS1⁹ written to correct polarization data in neutron elastic scattering. The modified program⁸ calculates the angular and energy dependence of cross section, polarization, and rotation angle parameters from scattering amplitudes calculated from an optical potential. The contribution of the Mott-Schwinger interaction to the scattering amplitudes was also included and the angular range allowable was extended down to angles as small as 0.1° . The cross sections have also been corrected for absorption of neutrons in the scatterer.

III. ANALYSIS AND DISCUSSION OF RESULTS

Final results for the cross sections and analyzing powers are shown in Figs. 4-7. The errors indicated are due to statistical uncertainties only.

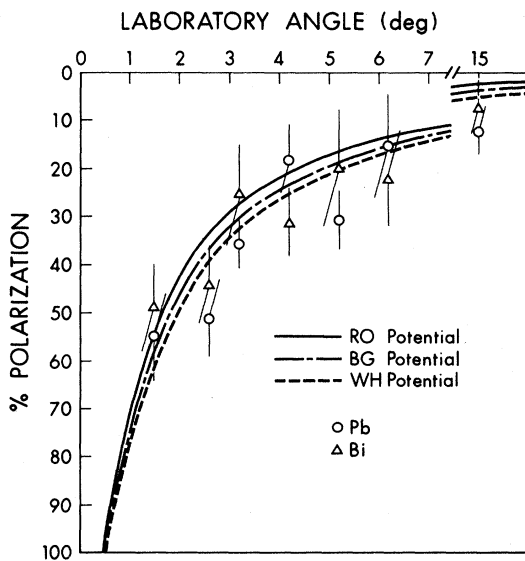


FIG. 4. Small angle analyzing power of 10 MeV neutrons scattered from Pb and Bi.

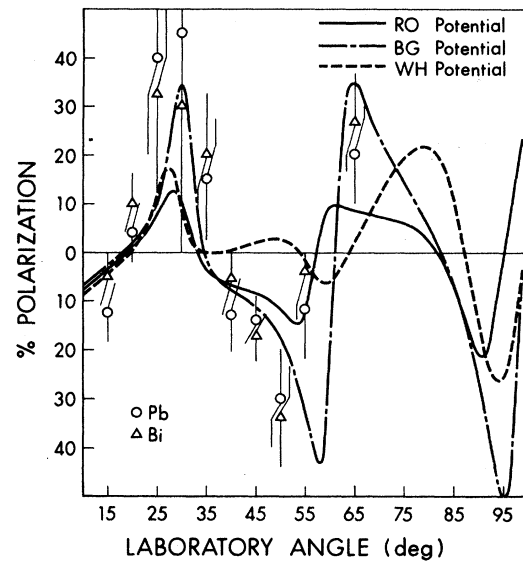


FIG. 5. Large angle analyzing power of 10 MeV neutrons scattered from Pb and Bi.

A comparison of the results of small angle measurements on Pb and Bi does not show any significant differences. This is in contrast to the situation reported by Drigo *et al.*⁴ at 2.45 MeV where a systematic variation was claimed. This does not rule out the possibility that the difference at 2.45 MeV is a real one. It would, therefore, be useful to repeat the experiment at 2.45 MeV and, if the differences reported are confirmed, to study further their energy dependence.

The cross sections and analyzing power of 10

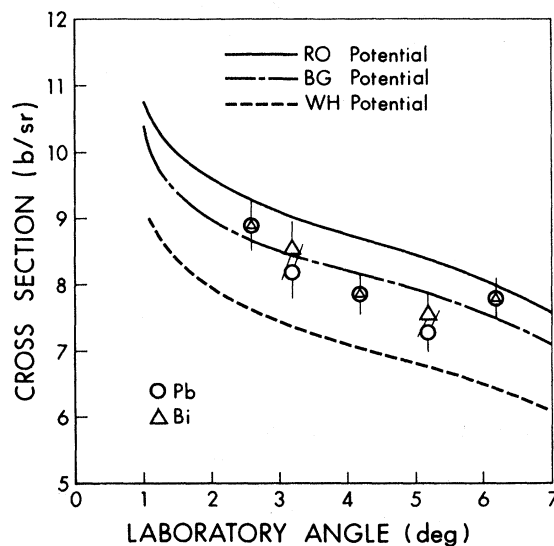


FIG. 6. Small angle cross section of 10 MeV neutrons scattered from Pb and Bi.

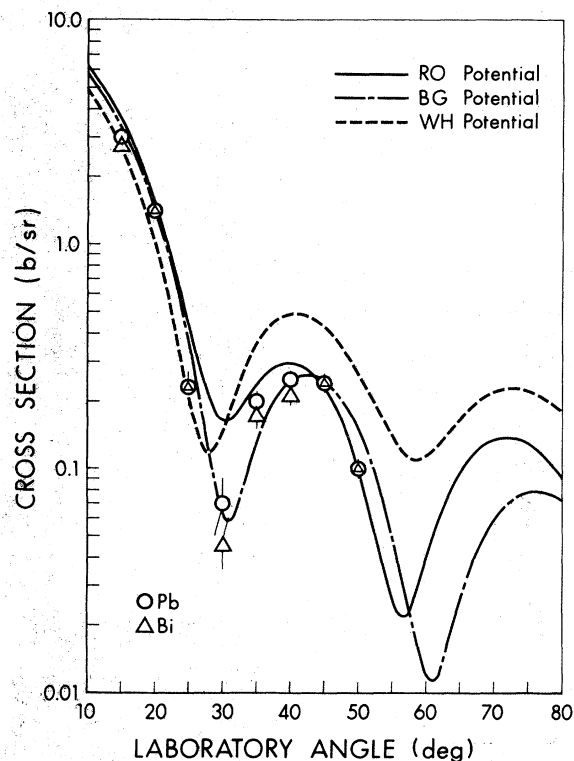


FIG. 7. Large angle cross section scattered from 10 MeV neutrons scattered from Pb and Bi.

MeV neutrons scattered from Pb have been calculated using a distorted-wave Born approximation (DWBA) approach¹⁰ in which the effect of the Mott-Schwinger interaction is treated as a perturbation. Optical potentials are used to calculate cross sections, polarizations, and reaction cross sections with and without the Mott-Schwinger interaction. The optical potential was defined as

$$U(r) = Vf(X_v) + i\left(W + 4a_w W_s \frac{d}{dX_w}\right) f(X_w) - 2(V_{so} + iW_{so}) \frac{1}{r} \frac{d}{dr} f(X_{so}) \vec{\sigma} \cdot \vec{L},$$

with

$$f(X) = (1 + e^X)^{-1}$$

and

$$X_i = \frac{r - r_i A^{1/3}}{a_i},$$

where i can be v , w , or so ; V , r_v , and a_v are the depth, radius, and diffuseness of the real part of the potential; W , W_s , r_w , and a_w are the volume depth, surface depth, radius, and diffuseness of the imaginary part of the potential; V_{so} , W_{so} , r_{so} , and a_{so} are the real depth, imaginary depth, radius, and diffuseness of the spin-orbit part of the poten-

tial; and $\vec{\sigma}$ and \vec{L} are spin and angular momentum operators.

Calculations have been made using three different sets of optical potential parameters. The three potentials used (Table I) are global potentials obtained by fitting scattering data for a large number of nuclei over a wide range of energies. The first potential, that of Rosen, Beery, and Goldhaber¹¹ (RO), is a local potential obtained by fitting polarization data. The second potential, that of Willmore and Hodgson⁶ (WH), is the local equivalence of the nonlocal potential of Perey and Buck,¹² and was generated by fitting cross-section data. The last potential, the Becchetti and Greenlees¹³ (BG) potential, is a local potential obtained by fitting cross sections and polarizations.

Where the Mott-Schwinger force dominates the interaction between the incident neutron and the scattering nucleus, only contributions from high partial waves will be significant. This means that the choice of the optical potential should have little effect on the magnitude of the analyzing power and the differential cross section in this region. In the case of scattering from heavy nuclei, this will hold true for angles less than 10° for the analyzing power measurements and below 2° for the cross section. This conclusion, as it applies to the analyzing power, has been confirmed by the present work. As shown in Fig. 4, the agreement between the measurements and theoretical calculation is good and there is little dependence on the optical potential used. Thus one can have confidence in the analyzing power predictions using the Mott-Schwinger interaction. This will facilitate the use of small angle scattering in neutron polarimeters. Galloway and Maayouf¹⁴ argued that a well designed

TABLE I. Optical model parameters used in the calculations.

Parameter	Rosen <i>et al.</i> ^a	Willmore and Hodgson ^b	Becchetti and Greenlees ^c
V (MeV)	46.30	44.22	48.02
r_v (fm)	1.25	1.26	1.17
a_v	0.65	0.65	0.75
W (MeV)	0.00	0.00	0.64
W_s (MeV)	5.75	4.22	7.98
r_w (fm)	1.25	1.24	1.26
a_w	0.70	0.48	0.58
V_{so} (MeV)	5.50	7.29	6.2
W_{so} (MeV)	0.00	0.00	0.00
r_{so} (fm)	1.25	1.22	1.01
a_{so}	0.65	0.65	0.75
σ_r (b)	2.82	1.90	2.95

^a Reference 11.

^b Reference 6.

^c Reference 13.

small angle polarimeter is as efficient as a helium polarimeter. With the confidence gained in the theoretical calculations, the small angle scattering polarimeter now has the advantage that the energy dependence of the analyzing power of the polarimeter can be accurately calculated.

The cross-section predictions for 10 MeV neutrons scattered from Pb or Bi at angles greater than 2° should, however, be sensitive to the choice of the optical potential. The BG potential produced the best fit to all the data presented in this work, while the RO potential fit, although not so good as the BG fit, is definitely better than the WH potential. Although all three potentials (Fig. 7) fitted the forward maximum of the large angle cross section data reasonably well, at the second maximum the BG potential provided a better fit. Moreover, the large angle analyzing power (Fig. 5) and small angle cross section (Fig. 6) are reproduced only by the BG potential predictions. This is in contrast to the results reported by Bucher and Hollands-

worth,⁵ who obtained a superior fit to the small angle scattering of 7–14 MeV neutrons from Pb and Bi using the WH potential compared to that obtained using the RO potential.

In conclusion, the present work indicates that only the nuclear and Mott-Schwinger interactions play an important role in the scattering of 10.4 MeV neutrons from Pb and Bi nuclei. Predictions of optical model calculations, when compared to the experimental data, show the best overall agreement can be obtained with the potential parameter set of Becchetti and Greenlees.

ACKNOWLEDGMENT

The authors wish to thank Dr. H. S. Sherif for very useful discussions and for the use of his computer program TASHTASH to perform the theoretical calculations. They would like also to thank Dr. W. K. Dawson for his on-line computer programs.

*This work was supported in part by the National Research Council of Canada.

†On leave of absence from the University of Alexandria, Egypt.

¹J. Schwinger, *Phys. Rev.* **73**, 407 (1948).

²G. V. Anikin and I. I. Kotukhov, *Yad. Fiz.* **12**, 1121 (1970) [*Sov. J. Nucl. Phys.* **12**, 615 (1971)].

³G. V. Gorlov, N. S. Lebedeva, and V. M. Morozov, *Yad. Fiz.* **8**, 1086 (1968) [*Sov. J. Nucl. Phys.* **8**, 630 (1969)]. F. T. Kuchnir, A. J. Elwyn, J. E. Monahan, A. Langsdorf, Jr., and F. P. Mooring, *Phys. Rev.* **176**, 1405 (1968).

⁴L. Drigo, C. Manduchi, G. Moschini, M. T. Russo-Manduchi, G. Tornielli, and G. Zannoni, *Nuovo Cimento* **13A**, 867 (1973).

⁵W. Bucher and C. E. Hollandsworth, *Phys. Lett.* **58B**, 277 (1975).

⁶D. Wilmore and P. E. Hodgson, *Nucl. Phys.* **55**, 673 (1964).

⁷D. C. DeMartini, C. R. Soltesz, and T. R. Donoghue, *Phys. Rev. C* **7**, 1824 (1973).

⁸A. H. Hussein, Ph.D. thesis, University of Alberta, Edmonton, Alberta, Canada, 1976 (unpublished).

⁹T. G. Miller, F. P. Gibson, and G. W. Morrison, *Nucl. Instrum. Methods* **80**, 325 (1970).

¹⁰H. Sherif, *Phys. Can.* **27**, 70 (1971).

¹¹L. Rosen, J. G. Beery, and A. S. Goldhaber, *Ann. Phys. (N.Y.)* **34**, 96 (1965).

¹²F. Perey and B. Buck, *Nucl. Phys.* **32**, 353 (1962).

¹³F. D. Becchetti, Jr., and G. W. Greenlees, *Phys. Rev.* **182**, 1190 (1969).

¹⁴R. B. Galloway and R. M. A. Maayouf, *Nucl. Instrum. Methods* **105**, 561 (1972).